

CW Operation of 1.55- μm Bipolar Cascade Laser With Record Differential Efficiency, Low Threshold, and 50- Ω Matching

Jonathan T. Getty, Erik J. Skogen, Leif A. Johansson, and Larry A. Coldren

Abstract—By electrically segmenting an InP ridge laser and series-connecting the segments, we have created the first highly scalable bipolar cascade lasers. We report room-temperature continuous-wave operation of 12-stage lasers with a record 390% differential efficiency and 2.8-mA threshold, as well as three-stage lasers with 50- Ω input impedance and 118% efficiency.

Index Terms—Bipolar cascade lasers, impedance matching, intergrated optoelectronics, ion implantation, optical amplifiers, quantum well (QW) intermixing, semiconductor lasers.

I. INTRODUCTION

DIFFERENTIAL QUANTUM EFFICIENCY (DQE), the ratio of photons emitted to electrons injected in a laser above threshold, can be of great importance in laser applications. High DQE is critical in direct modulation schemes, creating a large intensity variation with a small radio-frequency current. Efficiencies beyond unity allow a new class of devices that provide gain without a separate amplifier. This gain could be used to offset detector and coupling loss to make lossless taps (when modulated by a detector), to make amplifying wavelength converters (if the laser is tunable), or to avoid the noise of a separate amplifier.

DQE is conventionally limited (if a short cavity and/or antireflection (AR) coatings allow mirror transmission to dominate the losses) by injection efficiency, the fraction of electrons that recombine in the active region and participate in stimulated emission. While these can be improved with novel structures and materials, we rapidly approach the asymptotic limit of 100% injection. Further improvement in injection efficiency and DQE requires that the current pass through the device multiple times, or through multiple diodes sharing the same optical cavity. Past work [1]–[5] on these types of lasers, sometimes called a “bipolar cascade,” has been of limited success. Lasers employing two to four vertically stacked diodes, coupled by tunnel junctions, have proven useful in vertical cavity lasers, but have barely exceeded 100% DQE, and only at short wavelengths [1], [3] or under pulsed conditions [2].

We have pursued the technique, shown schematically in Fig. 1, of electrically segmenting a ridge laser along its length,

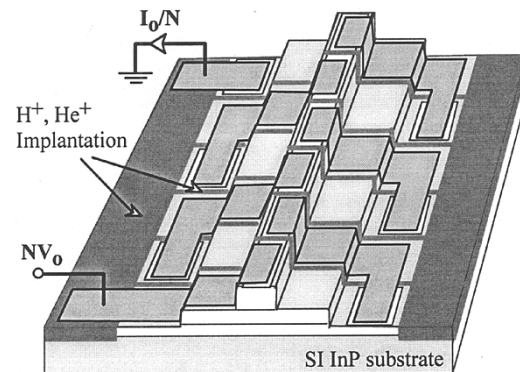


Fig. 1. Three-dimensional schematic of bipolar cascade segmented ridge laser. The dark grey areas are ion-implanted to force current, in series, through N diode stages.

series-connecting these segments, and driving the current through multiple diodes [4], [5]. Unlike the vertically stacked case, this laser can be scaled to a large number of stages without excessive epitaxy, allowing very large DQE, with small threshold currents. Terminal current passes, in turn, through each of the N diodes, creating the same current density with N times less current than a conventional single-contact laser. If this can be achieved without additional loss, threshold gain and current *density* will be unchanged, and threshold current is reduced by a factor of N . Above threshold, each electron of terminal current corresponds to N electron–hole pairs, enhancing DQE by the same amount. Voltage increases linearly with the number of stages, and resistance quadratically, reaching 50 Ω (an added benefit) in three to four stages. Input power is unchanged because the reduced current compensates the increased voltage and resistance (e.g., IV and I^2R). Such an idealized case requires optically transparent electrical isolation between stages, so we rely on ion implantation to eliminate interstage leakage, while minimizing the optical loss these implantations create.

II. CRITICAL TECHNOLOGY

In this case, a 3- μm -thick cross section is implanted from surface to substrate with a series of H^+ and He^+ isolation implants. These range from 20 to 240 keV for protons, and 55 to 1.2 MeV for He^+ , which is needed because protons do not effect sufficient damage in n-InP [6]. Doses were chosen to achieve a H–He density of at least $1 \times 10^{18} \text{ cm}^{-3}$, causing damage that

Manuscript received May 20, 2003; revised July 2, 2003. This work was supported by the Defense Advanced Research Projects Agency through the RF Lightwave Integrated Circuits (RFLICS) Program, and by the National Science Foundation.

The authors are with the Electrical and Computer Engineering Department, University of California, Santa Barbara, CA 93106 USA.

Digital Object Identifier 10.1109/LPT.2003.818646

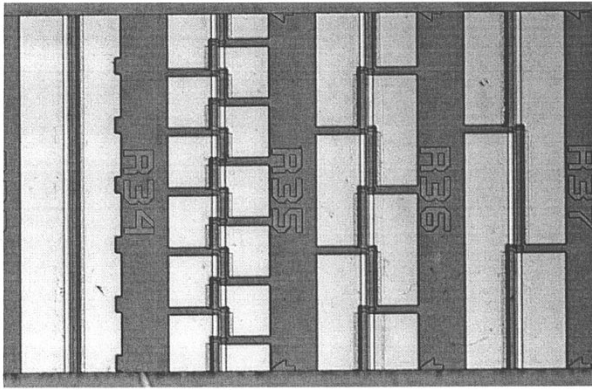


Fig. 2. Micrograph of a typical 600- μm laser bar. The laser on the left (R34) is a single-stage control laser. To its right are 12-stage (R35), 6-stage (R36), and 3-stage (R37) cascade lasers. The laser ridge itself is centered between each set of contacts.

reduces carrier lifetime and mobility to near-zero levels. Unfortunately, isolation implantation through the waveguide (to effect the underlying n-InP) affects the quantum wells (QWs) in the same way—these conditions also make for an ideal photon sink, since when light is absorbed by implanted QWs, the electron-hole pair instantly recombines nonradiatively. If nothing is done to prevent this, a 3- μm -long isolation implanted stripe, which electrically segments adjacent stages, will unbleachably absorb 40% of the light passing through it.

We avoided this problem by using implantation-induced QW intermixing (II-QWI) to passivate the QWs in the isolation stripe, blueshifting the absorption edge in this area to beyond the lasing wavelength. Modifying the technique pioneered by Charbonneau [7], we grow an undoped sacrificial layer above the waveguide, shallowly implant with $5 \times 10^{14} \text{ cm}^{-2}$, 100-keV P^+ to create defects near the surface, then anneal at 700 °C to drive these defects downward, intermixing the QWs in the P^+ -implanted regions. The sacrificial layer is etched down to an unblemished InP layer, a p-doped cap is regrown, and the sample is processed as described later.

Our intermixing method [8] eliminates the problem of Zn diffusion by conducting the blueshifting anneal before Zn is added to the structure, and stabilizes the intermixed material by immediately removing the source of the defects. This also allows us to separately optimize the intermixing conditions, rather than struggling to make them compatible with a preexisting p-doped cap. It is also notable that our process is compatible with distributed feedback and distributed Bragg reflector laser fabrication approaches, in which a similar regrowth step is required to bury a grating etched into the top surface of the quaternary waveguide.

III. PROCESS

The segmented laser was grown by metal-organic chemical vapor deposition (MOCVD) and uses a conventional ridge laser geometry and structure, with topside n-contacts on alternating sides of the ridge, as shown in Figs. 1 and 2. The active region of seven compressively strained InGaAsP 1.55- μm QWs is centered on a 4200- \AA waveguide of 1.3Q InGaAsP. This sits above 10 000 \AA of epitaxial n-InP, with a buried n^+ 1.1Q InGaAsP

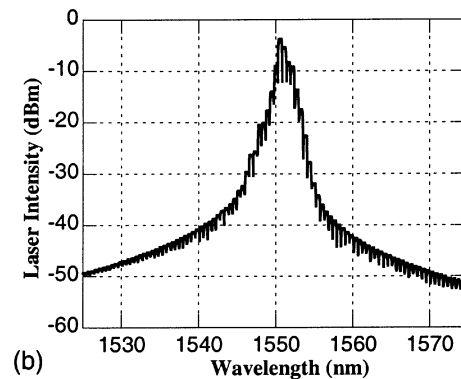
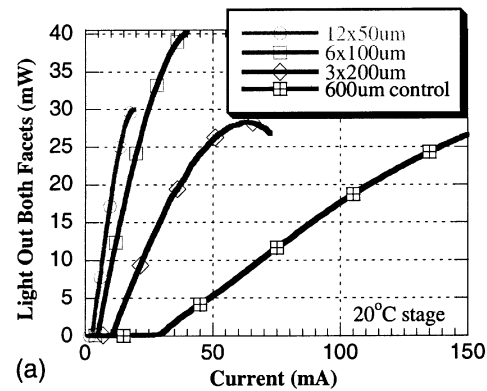


Fig. 3. (a) L - I response of a 600- μm laser, subdivided into 1, 3, 6, and 12 stages. DQE exceeds 100% in all but the control laser. (b) Spectrum of the six-stage laser. The multimode behavior is typical of Fabry-Pérot lasers, and the mode spacing corresponds to the 600- μm cavity length.

layer serving as an n-contact layer, and a (100) InP substrate that is Fe-doped to prevent interstage leakage under the laser. As mentioned earlier, the first growth concludes with a 4500- \AA undoped sacrificial InP layer for QWI, which is removed and replaced with a 20 000- \AA p-InP-InGaAs cap during MOCVD regrowth.

A 4- μm -wide laser ridge is etched down to the waveguide, then a centered 20- μm stripe is etched down to expose the n-contact layer. After Ni-AuGe-Ni-Au n-contacts are deposited and annealed, the sample is coated in SiN_x , and implanted with H^+ and He^+ to kill carrier lifetime between stages, through to the semiinsulating substrate. Next, the SiN_x is etched to open contact windows, and Ti-Pt-Au is evaporated and annealed to serve as a p-contact and interconnect layer. The samples were thinned, cleaved into 600- μm laser bars, and are not yet anti/high reflection (AR/HR) coated. The finished device, shown in Fig. 2, illustrates lasers with 1, 3, 6, and 12 stages.

IV. RESULTS

The lasers were soldered to an AlN heatsink and placed on a 20 °C stage. They were biased with a current source, and the light collected by an integrating sphere. The continuous-wave (CW) light output-current (L - I) characteristics of a 600- μm laser bar, divided into 3-, 6-, and 12-stage lasers is shown in Fig. 3. Each division into smaller stages multiplies the DQE and divides the threshold current by nearly the number of stages, scaling as shown in Fig. 4(a). This culminates in a 12-stage laser

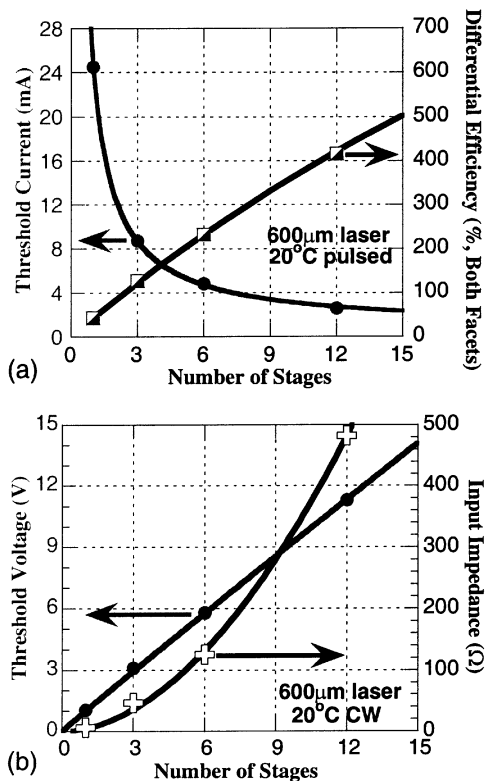


Fig. 4. Calculations of DQE, threshold conditions, and input impedance for 600- μm lasers, overlaid with experimental data. Pulsed measurements were used for DQE and threshold current to eliminate heating effects. CW measurements were used for voltage and resistance due to excessive voltage noise in pulsed measurements.

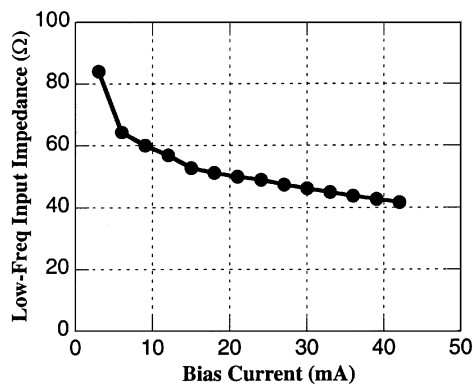


Fig. 5. Input impedance of the three-stage laser drops with current as dV/dI of the diode is reduced, reaching 50 Ω at a 21-mA bias.

with 50- μm stages, with 390% DQE and 2.8-mA threshold current. A longer laser, with 15 stages, reached 460% DQE. To our knowledge, this is the first demonstration of any 1.55- μm laser with CW DQE over 100%.

The drawback of multistage lasers is that higher voltages are required to drive many series-connected stages. Meanwhile, input impedance scales quadratically, as shown in Fig. 4(b). Fortunately, capacitance is reduced by the same amount, making the magnified resistance a benefit for impedance matching. The three-stage laser, which has 118% DQE and 9.9-mA threshold, has an input impedance that varies with bias

as shown in Fig. 5. It is nearly 50 Ω above threshold, while the threshold voltage is only 3.05 V.

Analysis of unsegmented control lasers has extracted several parameters of interest, which apply equally to the segmented lasers. Internal loss of 12.2 cm^{-1} is excellent for a seven-QW active region, and indicates that the Zn-free II-QWI process has eliminated a large source of optical loss without degrading the quality of the unshifted material. The injection efficiency of 69.4% is respectable but certainly an area for improvement. Curve fits indicate that the optical loss due to segmentation implants is 0.1–0.15 dB/segmentation, and could be slightly reduced; however, this is already better than the scattering loss caused by the more conventional passivation method of removing offset QWs, and regrowing InP.

V. CONCLUSION

We have demonstrated, for the first time, a highly scalable bipolar cascade laser with a conventional epitaxy and DQE several times higher than unity. This efficiency is ultimately limited by impractically high voltages and resistances, as well as by the finite length of the optically dead electrical segmentations. However, it is already high enough to drastically improve direct-modulation systems, or provide sufficient gain in photonic integrated circuits to offset significant fiber-coupling losses. The impedance of these lasers can be tuned to provide a broad-band match to any source impedance, by correctly choosing the number and length of stages. While this experiment used simple Fabry-Pérot ridge lasers, segmentation is compatible with most types of lasers, including tunable and active-passive designs.

REFERENCES

- [1] W. Schmid, D. Wiedenmann, M. Grabherr, R. Jäger, R. Michalzik, and K. J. Ebeling, "CW operation of diode-cascade InGaAs quantum well VCSEL," *Electron. Lett.*, vol. 34, pp. 553–555, 1998.
- [2] J. K. Kim, S. Nakagawa, E. Hall, and L. A. Coldren, "Near-room-temperature CW operation of electrically-pumped multiple-active-region 1.55- μm VCSELs with high differential efficiency," *Appl. Phys. Lett.*, vol. 77, pp. 3137–3139, 2000.
- [3] T. Knodl, M. Golling, A. Straub, and K. J. Ebeling, "Multi-diode cascade VCSEL with 130% differential quantum efficiency at CW room temperature operation," *Electron. Lett.*, vol. 37, pp. 31–33, 2001.
- [4] S. G. Ayling, D. R. Wight, M. B. Allenson, K. P. Hilton, and G. W. Smith, "Novel integrated laser devices with greatly enhanced quantum efficiency and intrinsic RF matching for low loss, broad band opto-microwave applications," in *Proc. SPIE Photonics West, Optoelectronics '98: Laser Diode Applications IV*, 1998, Paper 36, pp. 161–164.
- [5] J. T. Getty, O. Buchinsky, R. A. Salvatore, B. Mason, P. G. Piva, S. Charbonneau, K. S. Grabowski, and L. A. Coldren, "Monolithic series-connected 1.55 μm segmented-ridge lasers," *Electron. Lett.*, vol. 35, pp. 1257–1258, 1999.
- [6] S. J. Pearton, C. R. Abernathy, M. B. Panish, R. A. Hamm, and L. M. Lunardi, "Implant-induced high-resistivity regions in InP and InGaAs," *J. Appl. Phys.*, vol. 66, pp. 656–662, 1989.
- [7] S. Charbonneau, P. J. Poole, P. G. Piva, G. C. Aers, E. S. Koteles, M. Fallahi, J. J. He, J. P. McCaffery, M. Buchanan, M. Dion, R. D. Goldberg, and I. V. Mitchell, "Quantum-well intermixing for optoelectronic integration using high-energy ion implantation," *J. Appl. Phys.*, vol. 78, pp. 3697–3705, 1995.
- [8] E. J. Skogen, J. S. Barton, S. P. DenBaars, and L. A. Coldren, "A quantum well intermixing process for wavelength agile photonic integrated circuits," *IEEE J. Select. Topics Quantum Electron.*, vol. 8, pp. 863–869, July/Aug. 2002.